Assessment on the Progressive Collapse Resistance of a Long-Span Curved Spatial Grid Structure With Main Trusses

Guangpan Zhou (guangpanzhou@njust.edu.cn)
Nanjing University of Science and Technology
Qianen Song
Researcher of Nanjing Architectural Design and Research Institute Co., Ltd
Aiqun Li
Southeast University
Shungao Shen
Researcher of China Aviation Planning and Design Institute (Group) Co., Ltd.
Qing Zhou
Researcher of China Aviation Planning and Design Institute (Group) Co., Ltd.
Bin Wang
Nanjing University of Science and Technology
Yuye Zhang
Nanjing University of Science and Technology

Research Article

Keywords: long-span, spatial grid, truss, concrete, sensitivity analysis, progressive collapse

Posted Date: June 21st, 2021

DOI: https://doi.org/10.21203/rs.3.rs-632949/v1

Version of Record: A version of this preprint was published at KSCE Journal of Civil Engineering on December 27th, 2021. See the published version at https://doi.org/10.1007/s12205-021-5371-1.

Assessment on the Progressive Collapse Resistance of a Long-Span Curved Spatial Grid Structure with Main Trusses

Guangpan Zhou [a]*, Qianen Song [b], Aiqun Li [c, d], Shungao Shen [e], Qing Zhou [e], Bin Wang[f] and Yuye Zhang[g]

[a] Assistant Professor of School of Science, Nanjing University of Science and Technology, Nanjing 210094, China
[b] Researcher of Nanjing Architectural Design and Research Institute Co., Ltd., Nanjing 210014, China, songqianen1990@sina.cn
[c] Professor of School of Civil Engineering, Southeast University, Nanjing 210096, China, liaiqun@seu.edu.cn
[d] Professor of Beijing Advanced Innovation Center for Future Urban Design, Beijing University of Civil Engineering and Architecture, Beijing 100044, China
[e] Researcher of China Aviation Planning and Design Institute (Group) Co., Ltd., Beijing 100120, China, guangpan@illinois.edu (SG Shen); zhougqing@sina.com (Q Zhou)
[f] Master Candidate of School of Science, Nanjing University of Science and Technology, Nanjing 210094, China, binwang@njust.edu.cn
[g] Associate Professor of School of Science, Nanjing University of Science and Technology, Nanjing 210094, China, zyy@njust.edu.cn

Corresponding Author: Guangpan Zhou, School of Science, Nanjing University of Science and Technology, No. 200 Xiaolingwei Road, Nanjing 210094, China. Email: guangpanzhou@njust.edu.cn

Abstract: The present work is aimed at studying the progressive collapse resistance of the terminal building of Zhongchuan Airport in Lanzhou, China, which is a long-span curved spatial grid structure with main trusses. Firstly, the finite element model was built using MSC.Marc software. The alternate load path method (AP method) was used to simulate the initial failure of component. An improved method of zoned concept judgment and sensitivity analysis was proposed to determine the key components. Then, the initial failure components were removed individually on the course of analyzing. The responses of remaining structure were calculated using nonlinear dynamic analysis method. According to the results, the structure has a strong ability of resisting progressive collapse, though the structural responses are significant when removing the concrete filled steel tubular column directly supporting the roof at cantilever end. The maximum vertical displacement reaches 10 m. Moreover, the proposed method can avoid omitting the key components having significant influence on structural progressive collapse resistance. In addition, the influences brought by the cross-sectional sizes of chord and web members were investigated through conducting parametric analysis. The research can provide references for the structural optimization and safety control of similar long-span spatial structures.

Keywords: long-span; spatial grid; truss; concrete; sensitivity analysis; progressive collapse

1. Introduction

Nowadays, the structural collapse accidents occur frequently in China, resulting in huge casualties and economic losses, especially the collapses of public buildings with large pedestrian flow and complex structural forms, such as airport terminal buildings, railway station buildings, etc. The researches on the progressive collapse of building structures began from the collapse of Ronan Point Apartment Building in England in 1968, caused by the gas pipe explosion. Then, the collapse of Alfred P. Murrah Federal Building in America caused by the terrorist attack of car bomb in 1995 marked the beginning of the second research stage of progressive collapse. Corley et al. (1998) studied the collapse mechanism of Murrah Building and the measures that should be taken, and summarized the structural design process for reference. Longinow and Mniszewski (1996) discussed the damage mechanism of Murrah Building under the explosion, and put forward that the load can be redistributed to effectively prevent the continuous damage of statically indeterminate structure under bomb attack, such as steel frame and cast-in-place concrete frame. The third research stage of progressive collapse began from the 9/11 Incident. American Baker Engineering and Risk Consulting Co., Ltd. developed a computer program for building damage calculation and corresponding database for the U.S. Department of Defense.

Kaewkulchai and Williamson (2004) proposed a finite element program to simulate the progressive collapse process of frame structure. Marjanishvili and Agnew (2006) studied the advantages and disadvantages of the four calculation methods of alternate load path method (AP method), and summarized that the calculation methods of linear static, linear dynamic, and nonlinear dynamic are the three most effective analysis methods. The Eurocode 1, British code BS8110, U.S. code GSA2003, and DoD2010 specified the structural robustness, building safety classification, AP method, and tensile strength method, respectively (Eurocode 1, 2005).

China scholars began to conduct extensive related researches at the third research stage of progressive collapse. Zhang and Liu (2007) studied the evaluation methods of structural vulnerability and component importance under accidental loads. Hu and Qian (2008) researched the dynamic effects of a steel frame structure during progressive collapse process, and summarized the influencing laws of dynamic amplification coefficient. Ye et al. (2006) studied the progressive collapse of a reinforced concrete (RC) frame structure. Li et al. (2007) studied the influence of constraint conditions at column ends on the dynamic responses of frame columns under explosive impact using ANSYS software. Shi et al. (2007) studied the influence of initial damage on the collapse process of RC frame under explosion using LS-DYNA software. Li (2011), Cai et al. (2011) and Zhou et al. (2010) studied the design method of structural progressive collapse resistance, failure simulation using AP method, and the progressive collapse resistance of a practical projects, respectively. However, the progressive collapse mechanisms of different structural forms are diverse. The current researches mainly focus on the frame structures and simple large-span structures. For the complex structures, especially the complex large-span spatial structures composed of curved space grids and trusses, the research on the mechanism of progressive collapse resistance is still insufficient.

In this paper, the alternate load path method (AP method) was used to evaluate the progressive collapse resistance of the terminal building of Lanzhou Zhongchuan Airport in China, which is a long-span curved spatial grid structure with main trusses. The finite element model was built using MSC.Marc software adopting the fiber model based on material. The improved method of zoned concept judgment was proposed to preliminarily select the initial failure components. Then, the key components were determined through conducting sensitivity analysis, including the columns supporting the roof, columns of the RC frame, and web members of the main trusses. The key components were removed individually to evaluate the progressive collapse resistance of the structure. Finally, the parametric analyses of progressive collapse resistance were carried out, and the cross-sectional sizes of the chord and web members of grid structure close to the most critical component were selected as independent variables.

2. Project Overview

The Zhongchuan Airport is located in Lanzhou City, Gansu Province in China, which was opened to traffic in February 4, 2015. The global layout of terminal building is shown in Fig. 1(a), which can be divided into three parts with structural joints, including the middle part and the corridors on both sides. In this study, the progressive collapse resistance of the middle part shown in Fig. 1(b) was analyzed, which is a large-span curved spatial grid system with main trusses, including Grid parts A~D and Trusses I~III between grids. The structural form of the single grid unit is a quadrangular cone with a side length of 3 m and a height of 2 m. The grid members and truss members are made of round steel tubes and square steel tubes, respectively. The sectional view and plane layouts of roof and columns are shown in Fig. 1(c) and (d), respectively. As can be seen, the middle part is a super long structure with a length of

336 m and a width of 186 m. The length of cantilever segment at the end of roof is up to 24 m. The columns supporting the roof include concrete filled steel tubular (CFST) columns and steel tube columns, without lateral supports between columns.

In addition, a two-story RC frame structure is included by the middle part under the roof connected through columns, which can be divided into four independent parts with the plane dimensions of 105 m×24 m, 288 m×86 m, 72 m×24 m, and 68 m×79 m, respectively. The heights of the first and second floors are 3.8 m and 7.8 m, respectively. The columns of the frame include rectangular RC columns and circular CFST columns. The rectangular RC beams are adopted by the frame.

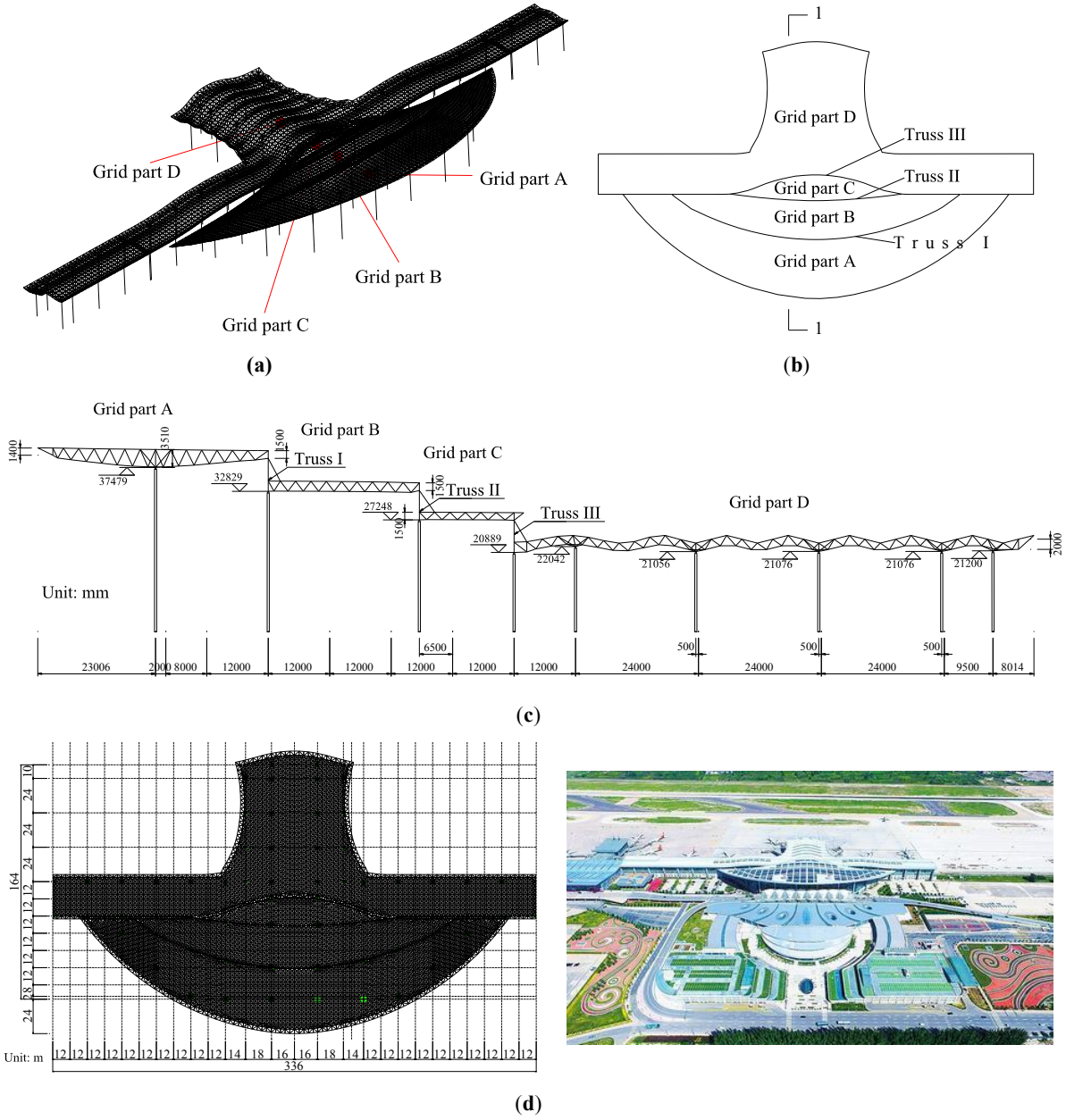

Fig. 1. Global layout of roof structure: **(a)** Isometric view; **(b)** Structural zones of middle part; **(c)** Profile 1-1; and **(d)** Plane layouts of roof and columns (the columns are shown in green color).

In general, the middle part of the terminal building is characterized by large column spacing, high column height, long cantilever length, and single transmission path of vertical force. The residual structure may not have enough backup load path to bear the load after the initial local damage caused by accident, resulting in progressive collapse of the structure. Moreover, the ticket hall with dense crowd is located in the middle part. The loss of life and property will be severe if the progressive collapse occurs.

Therefore, it is necessary to analyze the progressive collapse resistance of the structure.

3. Finite Element Model

The finite element model of the middle structure was established using the MSC.Marc software. The elastic shell element and spatial link element were used to simulate the floor and grid member, respectively. The material-based fiber model with high theoretical accuracy was adopted to simulate the column and beam, which can consider the influences of axial force and bending moment on the sectional hysteretic relationship. The fiber divisions of each kind of component are shown in Fig. 2, with assuming that each fiber was only subjected to axial force, and the deformation and stress characteristics of the cross-section were obtained by conducting integral for each fiber.

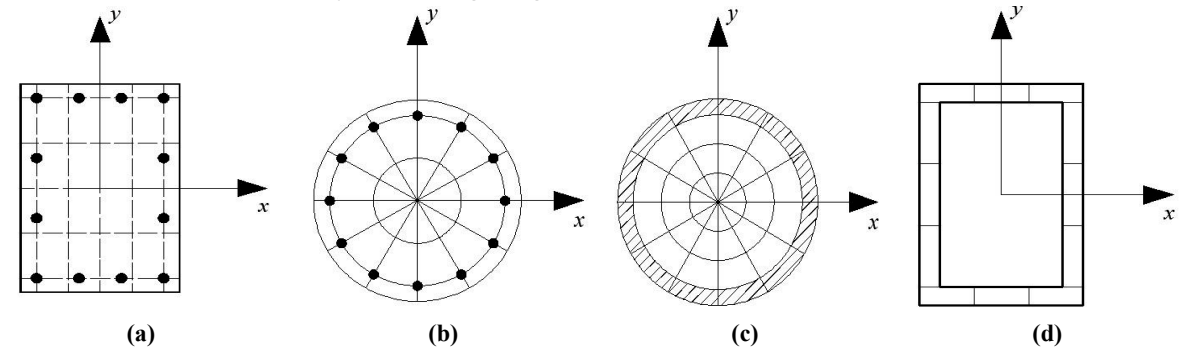

Fig. 2. Material-based fiber model of each kind of component: **(a)** RC with rectangular section; **(b)** RC with circular section; **(c)** CFST with circular section; and **(d)** Steel pipe with rectangular section.

The calculation accuracy of the fiber model depends on the selection of uniaxial hysteretic relationship. The constitutive relations of concrete and steel rebar in the Reference (Ye et al., 2006) were adopted. The behaviors of ordinary concrete, RC, and steel tube confined concrete can be simulated by modifying the ultimate compressive strength σ_u and compressive strain ε_u of concrete. In addition, the hysteresis model of compression constitutive relation of concrete is characterized by origin oriented type, the descending segment of the constitutive model is a straight line, and the rising segment is shown in Eq. (1),

$$\sigma = f_c[2(\frac{\varepsilon}{\varepsilon_c}) - (\frac{\varepsilon}{\varepsilon_c})^2] \tag{1}$$

where, σ and ε are the stress and strain of concrete, respectively; f_c and ε_c are the compressive yield strength and strain of concrete, respectively.

Moreover, the strength enhancement of concrete under the restraint of steel rebar or steel pipe was considered. The RC model proposed by Legeron and Paultre (2003) and the CFST model proposed by Han (2018) were used to calculate the peak compressive strength σ_{c0} and strain ε_{c0} of concrete fibers of the material-based fiber models shown in Fig. 2, as well as the ultimate compressive strength σ_{cu} and strain ε_{cu}.

The tensile constitutive model of concrete is shown in Eq. (2),

$$\begin{aligned} \sigma &= E_t\varepsilon && (\varepsilon \le \varepsilon_{t0}) \\ \sigma &= f_t \exp[-\alpha(\varepsilon - \varepsilon_{t0})] && (\varepsilon > \varepsilon_{t0}) \end{aligned} \tag{2}$$

where, E_t is the elastic modulus of concrete; f_t and ε_{t0} are the tensile yield strength and strain of concrete, respectively.

The constitutive model of steel rebar is shown in Eq. (3), and the monotonic loading curve of which is composed of three parts, including two straight line segments and one parabola segment. The

Bauschinger Effect of rebar is reasonably considered in the reloading path, which can reflect the yield, hardening, and softening effects of rebar.

$$\begin{aligned} \sigma &= E_s\varepsilon && (\varepsilon \le \varepsilon_y) \\ \sigma &= f_y && (\varepsilon_y < \varepsilon \le k_1\varepsilon_y) \\ \sigma &= k_4 f_y + \frac{E_s(1-k_4)}{\varepsilon_y(k_2-k_1)^2}(\varepsilon - k_2\varepsilon_y)^2 && (\varepsilon > k_1\varepsilon_y) \end{aligned} \tag{3}$$

where, E_s is the elastic modulus of steel rebar; f_y and ε_y are the yield strength and strain of rebar, respectively. k_1 is the ratio of hardening initial strain to yield strain, taking 4; k_2 is the ratio of peak strain to yield strain, taking 25; k_3 is the ratio of ultimate strain to yield strain, taking 40; k_4 is the ratio of peak stress to yield strength, taking 1.2.

The ideal elastoplastic bilinear hysteretic model in MSC.Marc software was used to simulate the constitutive model of steel member, as shown in Eq. (4). The symbol interpretations can be referred to those of rebar constitutive model.

$$\sigma = E_s\varepsilon,\ (\varepsilon \le \varepsilon_y)\ ;\ \sigma = f_y, (\varepsilon > \varepsilon_y) \tag{4}$$

The finite element model established by MSC.Marc software is shown in Fig. 3. The Midas model was established simultaneously for comparison and verification. The total weights of Midas model and Marc model are 80030 t and 80160 t, respectively, with a difference ratio of 0.16%, which can be ignored. The comparisons of the first ten natural vibration periods and the first three mode shapes calculated by the two models are shown in Table 1 and Fig. 4, respectively. The period differences are within reasonable range, and the first three mode shapes are the same.

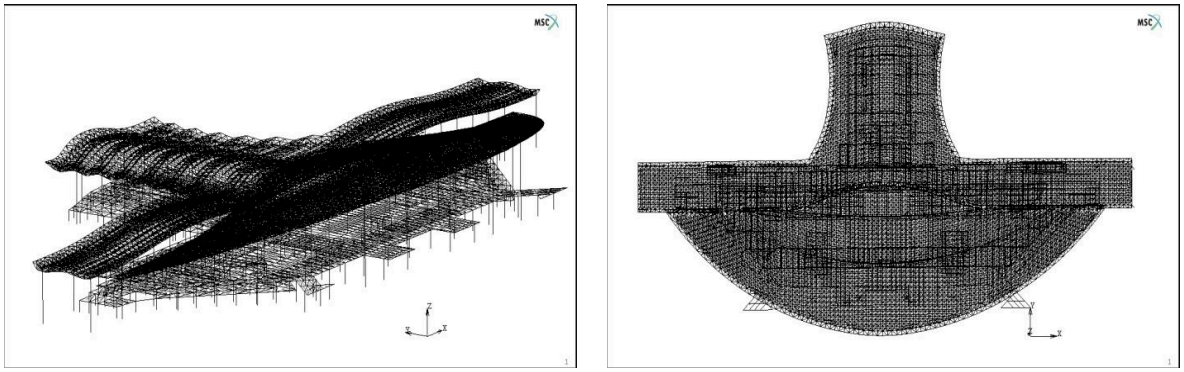

(a) **(b)**

Fig. 3. Finite element model established using Marc software: **(a)** 3D view; **(b)** Top view.

Table 1

Comparison of natural vibration period between Marc model and Midas model.

Order	Period (s)			Order	Period (s)		
	Midas model	Marc model	Error (%)		Midas model	Marc model	Error (%)
1	1.3575	1.2549	-7.56	6	0.8112	0.7634	-5.89
2	1.2745	1.2083	-5.19	7	0.6972	0.7189	3.11
3	1.2161	1.1388	-6.36	8	0.6607	0.7163	8.42
4	0.9858	0.9434	-4.30	9	0.655	0.7042	7.51
5	0.9631	0.9091	-5.61	10	0.6072	0.7032	15.81

Note: Error=[(value of Marc model–value of Midas model)/value of Midas model]×100.

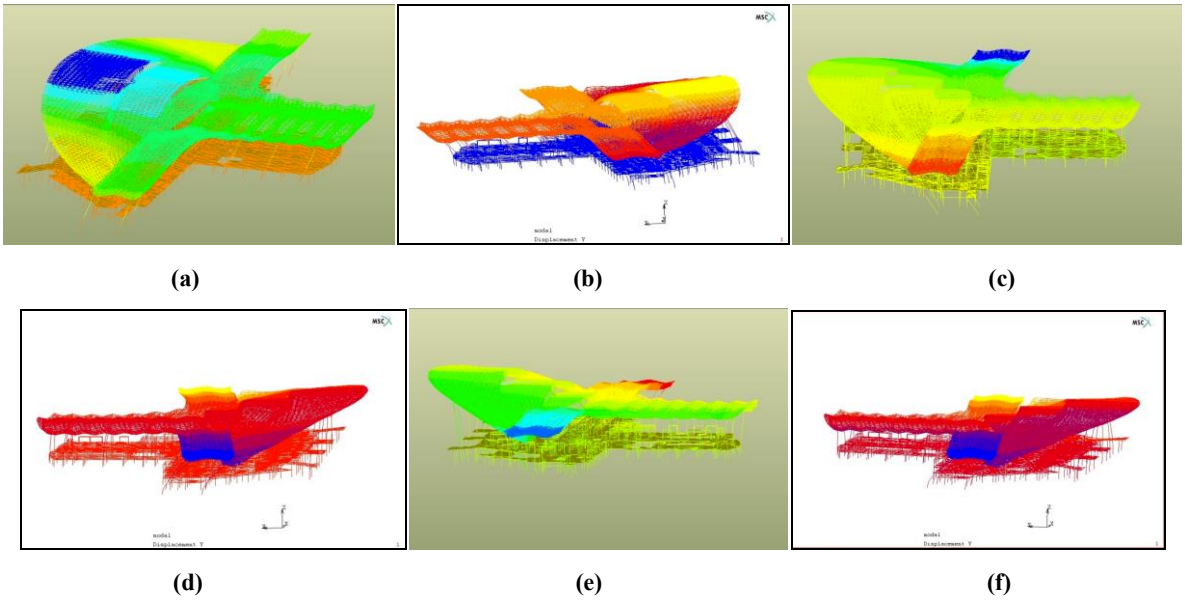

Fig. 4. Comparison of mode shape: **(a)** First mode shape of Midas model; **(b)** First mode shape of Marc model; **(c)** Second mode shape of Midas model; **(d)** Second mode shape of Marc model; **(e)** Third mode shape of Midas model; and **(f)** Third mode shape of Marc model.

4. Progressive Collapse Analysis Method

4.1. Alternate Load Path Method

The alternate load path method (AP method) was adopted to conduct the progressive collapse analysis of the structure. The subroutine "uactive" in Marc software controlling the life and death of element was used to simulate the instantaneous initial failure of component. The element was judged whether fails or not in the calculation process according to the failure criterion of material. Then, the subroutine uactive was used to "kill" the failed element. The failure process of related components caused by the overrun of stress and strain due to initial failure was calculated. Finally, the progressive collapse process of the structure was simulated.

4.2. Collapse Criterion and Failure Criterion

The structural progressive collapse and earthquake action are minimum probability events, so the latter factor was not considered in the progressive collapse analysis. Similarly, the wind load on the structure is small and randomly varying, which was also not considered in the calculation. The load combination of the structure during the progressive collapse calculation is as follows:

$$S = S_{GK} + 0.5\sum S_{qik} \tag{5}$$

where, S_{GK} is the standard value of permanent load; S_{qik} is the standard value of live load, including the snow load and the live loads on the roof and floor.

In the past, the indirect methods were generally used as the collapse criterion, such as the interlayer displacement angle exceeding 1/50, limited by the complex nonlinear dynamic process of structural collapse and development of computational means. However, the indirect criterion cannot reflect whether the structure really collapses or not. Now, the advanced nonlinear analysis tools have been able to accurately simulate the whole nonlinear dynamic process of structural collapse, including material nonlinearity and geometric nonlinearity. Therefore, the definition of structural collapse, "the structure loses the vertical bearing capacity and cannot maintain the living space to ensure the safety of person",

was taken as the structural collapse criterion in this study.

As for the failure criterion of member, the ultimate compressive strain of concrete fiber of the material-based fiber model simulating columns and beams was calculated according to the RC model proposed by Legeron and Paultre (2003). In addition, the ultimate tensile strain of steel rebar fiber was taken as 0.1. For the spatial link element simulating the grid member, the ultimate tensile strain and ultimate compressive strain were taken as 0.1. Moreover, the prevention goal of progressive collapse is that the remaining structural members will not crack and fall down. The members are allowed to maximize the bearing and deformation capacities, then, the standard values of material strength were adopted (Lu et al., 2008).

4.3. Determination Method of Initial Failure Component

The calculation conditions will be massive if considering the combined initial failure of multiple members for the long-span spatial structures, and it is unrealistic to analyze each condition. Therefore, the commonly used method in national codes was adopted, only the single initial failure of one component was considered in each analysis process. Moreover, it is time-consuming and unnecessary to simulate the initial failure of every component because of their different importance to structure. The method of concept judgment plus sensitivity analysis (Legeron and Paultre, 2003) was usually used to select the members having greater impacts on structure after failure, which are called "key components". Firstly, the relatively important components were preliminarily selected as initial failure components through concept judgment, then the key components were determined by conducting sensitivity analysis. However, the effectiveness of sensitivity analysis depends on the consistency of structural form. The sensitivity analysis results of different components can only be comparable when the components belongs to the same structural form. Moreover, the spatial forms of different roof parts of the terminal building in this study are different. Therefore, the improved method of zoned concept judgment plus sensitivity analysis was proposed to determine key components. The main steps are as follows:

(1) The structure was divided into different areas according to different structural systems or different spatial forms within the same structural system;

(2) The components were divided into different types according to their mechanical characteristics;

(3) For the different types of components in each area, the preliminary selection of initial failure components was determined by concept judgment;

(4) The sensitivity analyses were conducted for the preliminarily selected components, and the key components of each type were determined for each area, which were considered as the key components for the whole structure.

4.4. Sensitivity Analysis Method

The change of structural response caused by initial failure is defined as sensitivity, which is inversely proportional to the structural redundancy (Cai et al., 2011). The sensitivity analysis steps are as follows:

(1) The removal of initial failure member was selected as the damage parameter β for the structure;

(2) Calculate the sensitivity index S_{ij} of component i after applying the damage parameter β_j, namely, the initial failure component j was removed,

$$S_{ij} = (\gamma - \gamma') / \gamma \tag{6}$$

where, γ and γ' are the responses of nodes or elements of the original structure and damaged structure, respectively.

(3) Calculate the importance coefficient α^j. When the displacement response of node is taken as the object of sensitivity analysis, the formula of α^j is as follows,

$$\alpha^j = \sum_{i=1}^{n} \frac{|S_{ij}|}{n} \tag{7}$$

where, n is the total node number of the remaining structure after removing the initial failure component j.

In addition, when the overall response of the structure is taken as the object of sensitivity analysis, such as the bearing capacity and natural vibration period, the formula of α^j is as follows,

$$\alpha^j = |S_j| \tag{8}$$

where, S_j is the sensitivity index of the whole structure corresponding to damage parameter β_j.

5. Results and Discussions of Progressive Collapse Analysis

The components on the vertical load path of the structure were focused on during the selection of key components. Moreover, the single failure of one grid member will not greatly affect the structure because of the high degrees of indeterminacy and redundancy of grid structure, which was ignored during selecting key components. Therefore, the initial failure components of the structure include the columns directly supporting the roof, the columns of the RC frame, and the web members of the main trusses.

5.1. Column Supporting the Roof

5.1.1. Initial Failure Components

The vertical load on the failed column supporting the roof will be redistributed to the surrounding columns. The bending moments and shear forces of the grid members close to the failed column will increase and exceed the bearing capacity due to the change of supporting mode, resulting in the failures of grid members and even the progressive collapse of the roof. Therefore, the columns supporting the roof should be regarded as key components. During the concept judgment of key columns, the middle structure was divided into three areas as shown in Fig. 5, including Area I, II, and III. The columns with typical positions in each area were preliminarily selected as initial failure columns, including the corner columns, side columns, and inner columns. The cross-sectional sizes and material parameters of the preliminarily selected columns are shown in Table 2, which were numbered as SC1~SC16, including circular CFST columns and square steel pipe columns.

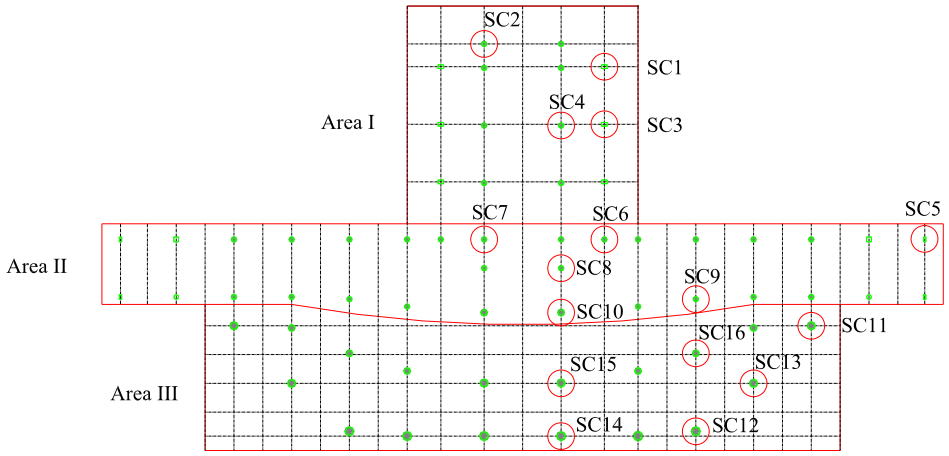

Fig. 5. Structural areas and preliminarily selected initial failure columns supporting the roof (in red circles).

Table 2

Geometric and material parameters of the preliminarily selected columns supporting the roof.

Area	Serial number	Column type	Sectional size (mm)	Steel material	Concrete material
Area I	SC1	Square steel pipe column	1200×800×25×35	Q345C	——
	SC2	Circular CFST column	Φ1200×20	Q345B	C60
	SC3	Square steel pipe column	1200×800×25×35	Q345C	——
	SC4	Circular CFST column	Φ1200×20	Q345B	C60
Area II	SC5	Square steel pipe column	1000×500×30×30	Q345C	——
	SC6	Circular CFST column	Φ1200×20	Q345B	C60
	SC7	Circular CFST column	Φ1200×20	Q345B	C60
	SC8	Circular CFST column	Φ1200×20	Q345B	C60
	SC9	Circular CFST column	Φ1200×20	Q345B	C60
	SC10	Circular CFST column	Φ1500×30	Q345B	C60
Area III	SC11	Circular CFST column	Φ1800×35	Q345C	C60
	SC12	Circular CFST column	Φ2000×40	Q345C	C60
	SC13	Circular CFST column	Φ1800×35	Q345C	C60
	SC14	Circular CFST column	Φ2000×40	Q345C	C60
	SC15	Circular CFST column	Φ1800×35	Q345B	C60
	SC16	Circular CFST column	Φ1500×30	Q345B	C60

The sensitivity analyses were carried out for the preliminarily selected columns supporting the roof. The dynamic amplification effect and material nonlinearity were not considered. The object of sensitivity analysis was node displacement. The calculated results of importance coefficients α^j are shown in Table 3. In order to avoid the influence of different roof form in each area, so that the component selection of different areas were not comparable, the relatively important columns with the importance coefficients exceeding 1.5 in each area, shown in bold, were regarded as the key components for progressive collapse analysis, including SC1, SC10, SC11, SC14, and SC15.

Table 3

Important coefficients of the preliminarily selected columns supporting the roof.

Area	Column supporting the roof	
	Serial number	Importance coefficient α^j
Area I	SC1	5.332
	SC2	0.575
	SC3	0.712
	SC4	0.636
Area II	SC5	0.466
	SC6	0.419
	SC7	0.359
	SC8	0.596
	SC9	0.389
	SC10	1.717
Area III	SC11	1.911
	SC12	1.000
	SC13	1.408
	SC14	3.993
	SC15	2.121
	SC16	0.824

5.1.2. Progressive Collapse Analysis Results

The progressive collapse resistance of the structure after removing the key columns SC1, SC10, SC11, SC14, and SC15 individually was studied using the AP method. The nonlinear dynamic

time-history analysis was carried out for the remaining structure. The final deformation of the structure, distribution of plastic members, and the vertical displacement curve of the node connecting the initial failure column and roof are obtained, as shown in Fig. 6~10.

The final deformation of the structure after removing column SC1 is shown in Fig. 6(a). The maximum vertical displacement of the cantilever end close to SC1 is 1.95 m. The members in blue color shown in Fig. 6(b) represent the members entering into plasticity. The vertical displacement curve of the node connecting SC1 and the roof is shown in Fig. 6(c). The first 1 s represents the application of initial load on the structure. The column SC1 was removed at 1.01 s to simulate the initial failure. The vertical deformation of the structure reaches the maximum at 2.15 s. Then, the structural vibration gradually weakens and finally stabilizes due to the damping effect. The failure of SC1 will not cause the progressive collapse of the structure.

Analogously, as shown in Fig. 7, only a small number of grid chords enter into plasticity after the removal of SC10, which has little impact on the structure and will not cause progressive collapse. As shown in Fig. 8, the initial failure of SC11 has a greater impact on the structure compared with that of SC10. More grid chords enter into plasticity, and there is also no progressive collapse of the structure. As shown in Fig. 9, the maximum vertical displacement of the adjacent cantilever end reaches 10 m after the removal of SC14. Most of the grid members around SC14 enter into plasticity. The lower chords included in the red box shown in Fig. 9(b) quit working due to reaching the ultimate tensile strain. Fig. 9(c) shows the side view of the failed lower chords. The structural constraints at SC14 are greatly reduced due to the destruction of a row of lower chords, and the structure is on the verge of collapse. As shown in Fig. 10, the vertical deformation of the structure is very small after the removal of SC15, and only a few members enter into plasticity.

To sum up, the structural responses after the removal of SC14 are the largest, and the structure is on the verge of collapse. However, the structural responses are small when other columns are removed, which reflects that the structure has enough backup load path and strong ability to resist progressive collapse.

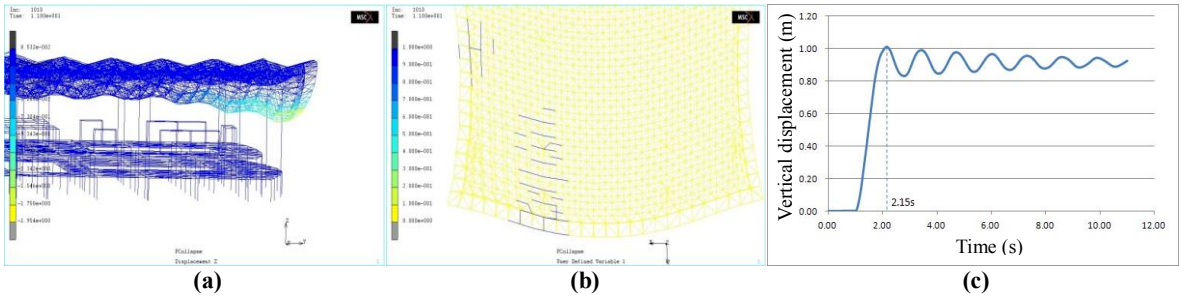

(a) **(b)** **(c)**

Fig. 6. Structural response after removing the initial failure column SC1: **(a)** Final deformation; **(b)** Distribution of plastic members (in blue color); and **(c)** Vertical displacement curve of the node connecting the roof and SC1.

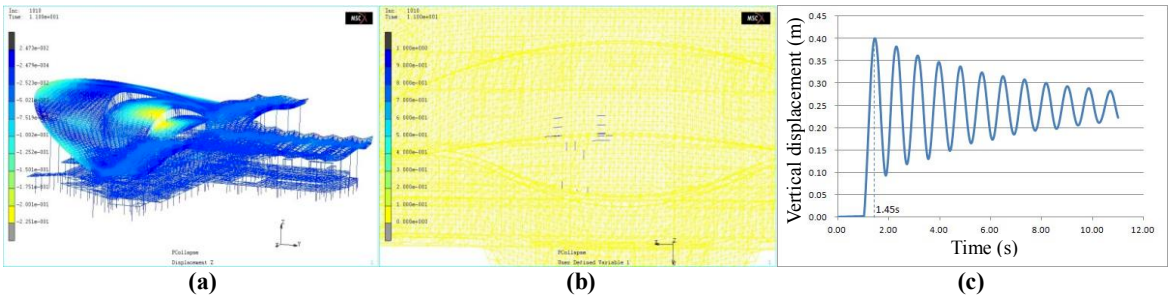

(a) **(b)** **(c)**

Fig. 7. Structural response after removing the initial failure column SC10: **(a)** Final deformation; **(b)** Distribution of plastic members (in blue color); and **(c)** Vertical displacement curve of the node connecting the roof and SC10.

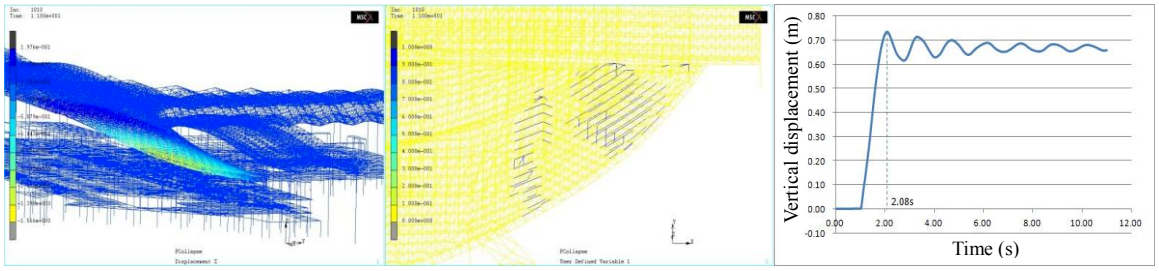

(a) **(b)** **(c)**

Fig. 8. Structural response after removing the initial failure column SC11: **(a)** Final deformation; **(b)** Distribution of plastic members (in blue color); and **(c)** Vertical displacement curve of the node connecting the roof and SC11.

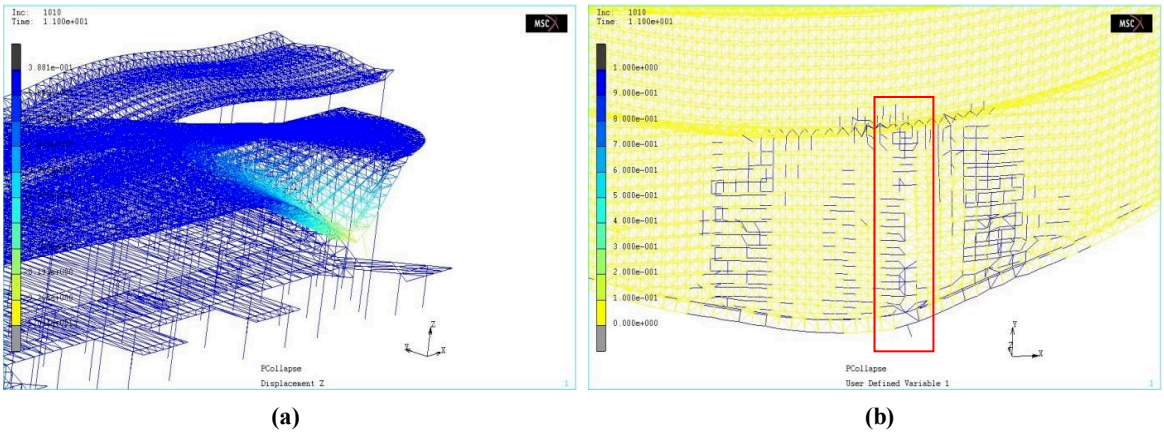

(a) **(b)** **(c)** **(d)**

Fig. 9. Structural response after removing the initial failure column SC14: **(a)** Final deformation; **(b)** Distribution of plastic members (in blue color, top view); **(c)** Distribution of failed lower chords (included in the light blue circle, side view); and **(d)** Vertical displacement curve of the node connecting the roof and SC14.

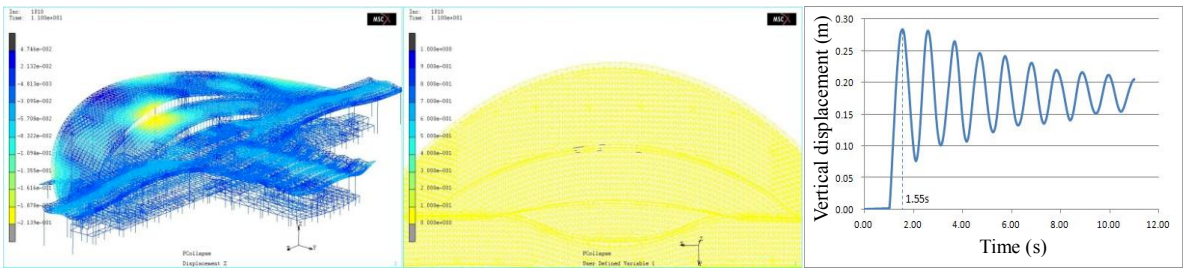

(a) **(b)** **(c)**

Fig. 10. Structural response after removing the initial failure member SC15: **(a)** Final deformation; **(b)** Distribution of plastic members (in blue color); and **(c)** Vertical displacement curve of the node connecting the roof and SC15.

In addition, the typical structural responses after the removals of SC1 and SC14 are shown in Table 4. As can be seen from Table 3 above, the importance coefficient α^j of SC1 is greater than that of SC14, which are 5.332 and 3.993, respectively. However, the structural responses after the initial failure of SC14 are greater than those of SC1 according to the results in Table 4. Namely, the column SC14 is more important to the progressive collapse resistance of the structure compared with SC1, which reflects that the actual importance of component in different area is not positively correlated with the importance coefficient α^j. Therefore, the complex structure should be divided into different areas before conducting sensitivity analysis. Moreover, the proposed method of zoned concept judgment plus sensitivity analysis in this study can effectively avoid the omission of key components.

Table 4

Typical structural responses after removing the key components of SC1 and SC14.

Serial number of initial failure column	Importance coefficient of column	Final vertical displacement of the top node of column (m)	Final number of yield component	Final number of failed component
SC1	5.332	1.01	55	0
SC14	3.993	3.96	590	16

5.2. Column of the RC Frame

5.2.1. Initial Failure Components

The columns of the two-story RC frame include RC columns and CFST columns, which play different roles in the vertical force transmission path because of their different locations. For the initial failure conditions of the RC columns, even if the frame beams and upper floor supported by a failed column are damaged and lose the abilities to bear vertical loads, the scope of damage is only limited to the part where the failed RC column is located. The vertical force transmission path of other parts of the frame does not change, and there is no significant impact on the columns directly supporting the roof, Therefore, the failures of RC columns of the frame was not considered during the progressive collapse analysis of the structure.

However, for the initial failure condition of CFST column of the frame, the column supporting the roof directly above the frame slab will be only supported by the frame beams. Then, the column supporting the roof might lose the ability to bear vertical loads due to the loss of support if the frame beams and slab failed. Moreover, the vertical force transmission path of the grid structure will change correspondingly, which is equivalent to the failure of the column directly supporting the roof. Namely, the failure influence of CFST column is more significant and may lead to the occurrence of progressive collapse, which should be regarded as key component. The preliminarily selected CFST columns of the frame are shown in Table 5, which are characterized by the same locations as the preliminarily selected columns supporting the roof.

Table 5

Preliminarily selected CFST columns of the frame.

Area	Serial number	Failure position of the CFST column	Area	Serial number	Failure location of the CFST column
Area I	FC2	First floor part	Area II	FC8-2	Second floor part
	FC4-1	First floor part		FC9	First and second floor parts
	FC4-2	Second floor part		FC10	First and second floor parts
Area II	FC6-1	First floor part	Area III	FC14	First and second floor

			parts
FC6-2	Second floor part	FC15-1	First floor part
FC7-1	First floor part	FC15-2	Second floor part
FC7-2	Second floor part	FC16-1	First floor part
FC8-1	First floor part	FC16-2	Second floor part

Note: the frame structure at column FC2 only has the first floor; the first and second floors at columns FC9, FC10, and FC14 are interconnected. Moreover, the CFST columns SC1, SC3, SC5, SC11, SC12, and SC13 in Fig. 5 do not support the frame structure.

The sensitivity analyses were carried out for the preliminarily selected CFST columns of the two-story frame. The calculated results of important coefficients α^j are shown in Table 6. The relatively important columns in each area with the importance coefficients exceeding 1.5 were regarded as key components for the progressive collapse analysis, including FC10, FC14, and FC15-1.

Table 6

Important coefficients of the preliminarily selected CFST columns of the frame.

Area	CFST column of the frame	
	Serial number	Importance coefficient α^j
Area I	FC2	0.415
	FC4-1	0.376
	FC4-2	0.428
Area II	FC6-1	0.450
	FC6-2	0.379
	FC7-1	1.278
	FC7-2	0.928
	FC8-1	1.366
	FC8-2	0.834
	FC9	0.563
	FC10	1.684
Area III	FC14	6.313
	FC15-1	2.194
	FC15-2	1.244
	FC16-1	0.619
	FC16-2	0.387

5.2.2. Progressive Collapse Analysis Results

The key CFST columns FC10, FC14, and FC15-1 of the frame were instantaneously removed individually using the AP method. The final structural deformation and distribution of plastic members are obtained as shown in Fig. 11. Where, the columns included in the light blue ellipses in Fig. 11(a), (c), and (e) represent the initial failure columns. The members in blue color in Fig. 11(b), (d), and (f) represent the members entering into plasticity.

As shown in Fig. 11(a)~(b), the vertical deformation of the structure after the removal of FC10 is very small, only the ends of few beams and columns enter into plasticity, and the roof members do not yield. As shown in Fig. 11(c)~(d), the structural vertical deformation is also very small after the removal of FC14. Only a few of beams and columns yield, the other parts of the structure do not enter into plasticity, and there is also no collapse. As shown in Fig. 11(e)~(f), the vertical displacements of the upper columns supporting the roof are larger compared with the adjacent CFST columns of the frame after removing FC15-1, but the absolute values of displacements are small. Moreover, the structure does not collapse and no member enters into plasticity.

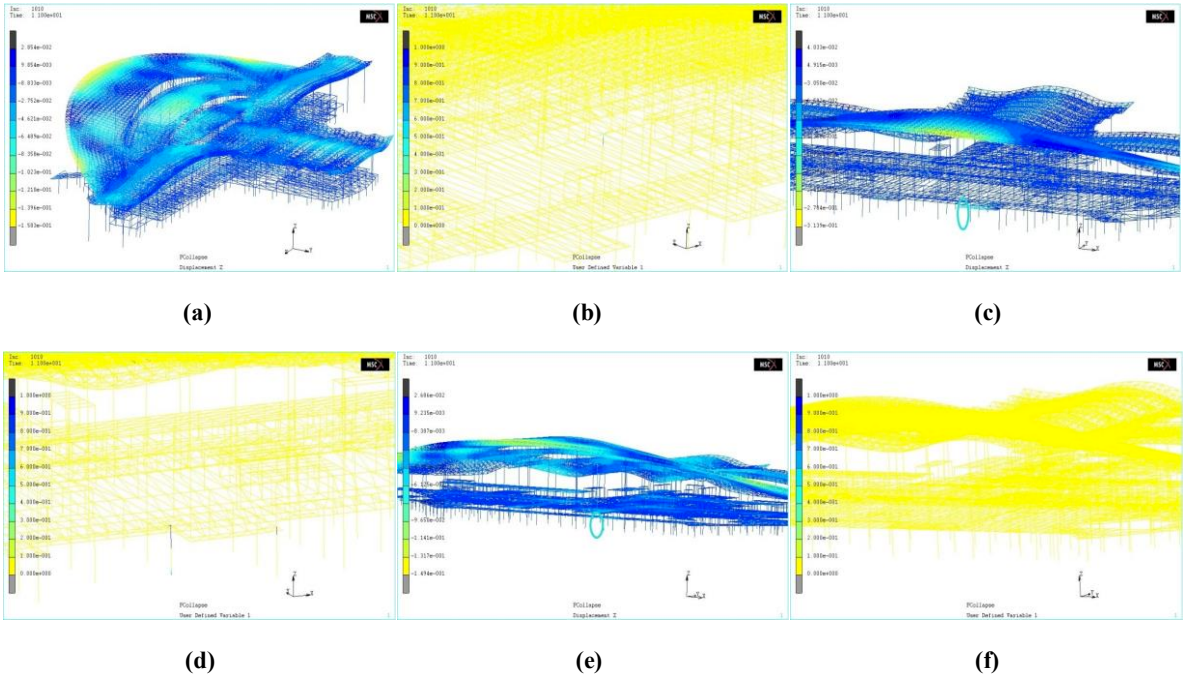

(a) **(b)** **(c)**

(d) **(e)** **(f)**

Fig. 11. Final deformation and distribution of plastic members after removing the initial failure CFST column of the frame: **(a)**~**(b)** FC10; **(c)**~**(d)** FC14; and **(e)**~**(f)** FC15-1.

5.3. Web Member of the Main Truss

5.3.1. Initial Failure Components

The main trusses are located at the junctions of adjacent curved grid structures with different heights, which are important parts to transfer the vertical loads of the upper grid layer to the CFST columns supporting the lower grid layer. Therefore, the vertical web members of the main trusses should be considered in the selection of key components. The three main trusses I~III have certain similarity, and the web members can be divided into ordinary web members and the web members directly connected with CFST columns. Therefore, the two representative web members of each truss were selected for progressive collapse analysis as shown in Fig. 12, including the web member in the middle of each truss (Rods I-1, II-1, and III-1) and the web member connected with the middle CFST column (Rods I-2, II-2, and III-2).

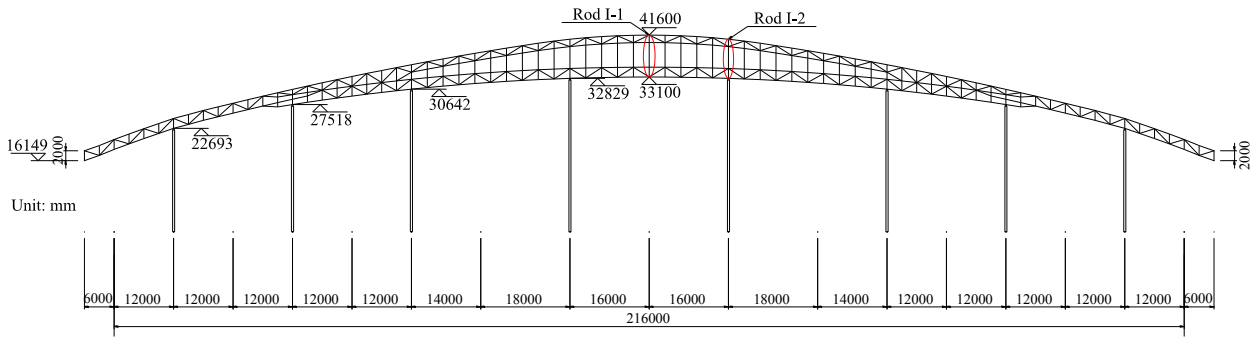

(a)

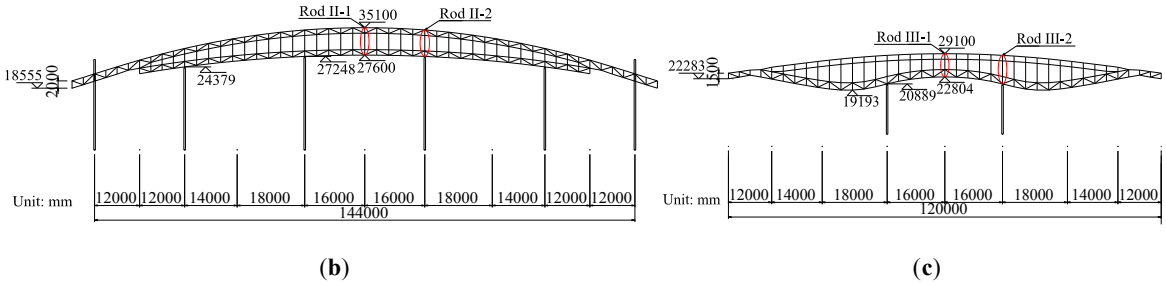

(**b**) (**c**)

Fig. 12. Initial failure web members of the trusses (in the red ellipses): **(a)** Truss I; **(b)** Truss II; and **(c)** Truss III.

5.3.2. Progressive Collapse Analysis Results

The final structural deformation and distribution of the members entering into plasticity are shown in Fig. 13. Where, the members included in the light blue ellipses represent the initial failure web members. As can be seen from the calculated results of Trusses I and II shown in Fig. 13(a)~(h), the removals of the web members directly connected with CFST columns, including Rods I-2 and II-2, have greater impacts on the structure compared with the ordinary web members Rods I-1 and II-1. Only a small number of members enter into plasticity, and the structure does not collapse. As shown in Fig. 13(i)~(l), the removals of Rods III-1 and III-2 of Truss III have little effect on the structure, no members enter into plasticity, and the structure does not collapse.

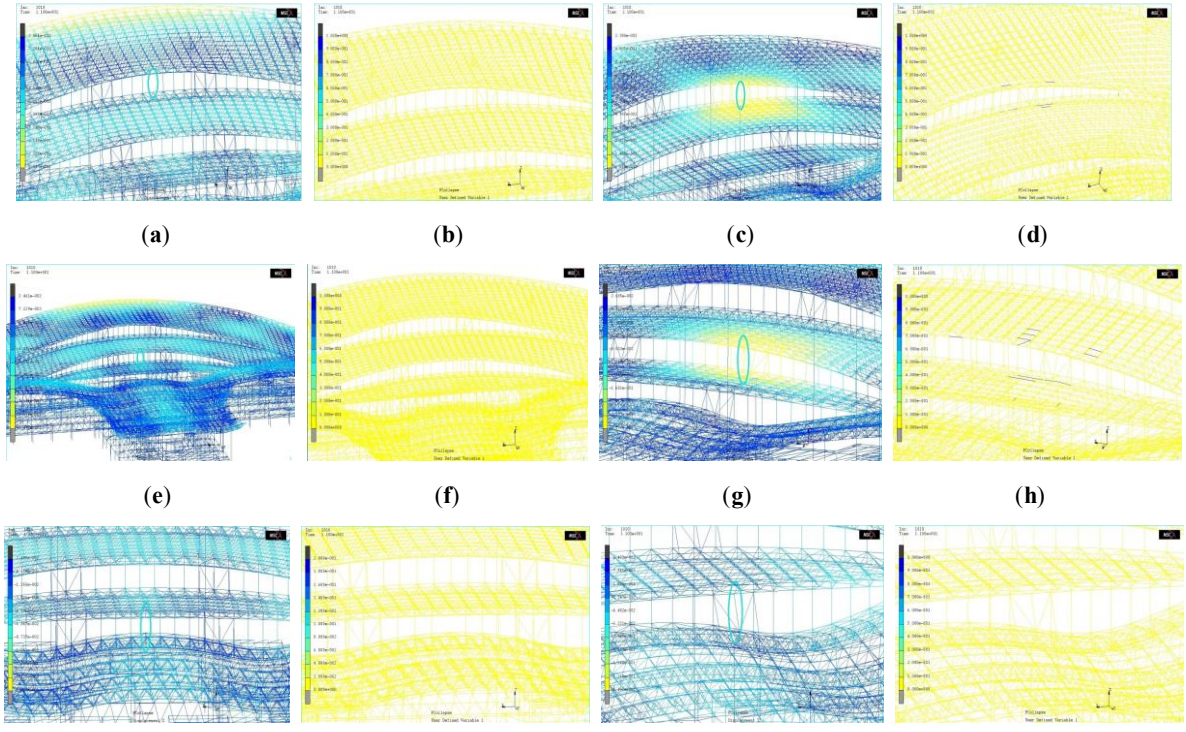

(**a**) (**b**) (**c**) (**d**)

(**e**) (**f**) (**g**) (**h**)

(**i**) (**j**) (**k**) (**l**)

Fig. 13. Final deformation and distribution of plastic members after removing the initial failure web members of the trusses: **(a)~(b)** Rod I-1; **(c)~(d)** Rod I-2; **(e)~(f)** Rod II-1; **(g)~(h)** Rod II-2; **(i)~(j)** Rod III-1; and **(k)~(l)** Rod III-2.

Conclusions can be drawn from the above analysis, the structural responses are the largest when the columns supporting the roof are selected as initial failure components, and otherwise the structural responses are small. Namely, the main cause of progressive collapse of the structure is the failure of the column supporting the roof, which will results in significant change in the supporting mode of grid structure, including the decrease of support points and increase of span. Then, the grid members in the

damaged area may yield or even fail due to the sharp change of stress, which will lead to the redistribution of internal force and failures of other members, and finally lead to the progressive collapse of the structure.

6. Parametric Analysis of Progressive Collapse Resistance

Most chord members of the grid structure close to the initial failure components will yield when the structure is in critical collapse according to the above calculated results, while the web members of grid structure rarely yield. In order to study the influences of the resistances of chord and web members on the progressive collapse resistance of the structure, the cross-sectional sizes of the chord and web members of grid structure were selected as independent variables. The amplification factors of member sectional area were 1.05, 1.10, 1.15, 1.20, 1.30 1.40, and 1.50, respectively. Moreover, because the structural responses after the removal of CFST column SC14 supporting the roof are the largest, and the structure is on the verge of collapse, SC14 was selected as the initial failure component of parametric analysis. The range for adjusting the cross-sectional sizes of chords and webs is shown in Fig. 14, which exactly includes all the grid members entered into plasticity or failed when the initial failure component was SC14. In addition, the vertical displacements of the four nodes supported by column SC14 were selected as the dependent variables, including the nodes numbered as 6715, 6644, 1916, and 6652 in the Marc model, as well as the vertical displacement of Node 8297 between SC14 and the roof.

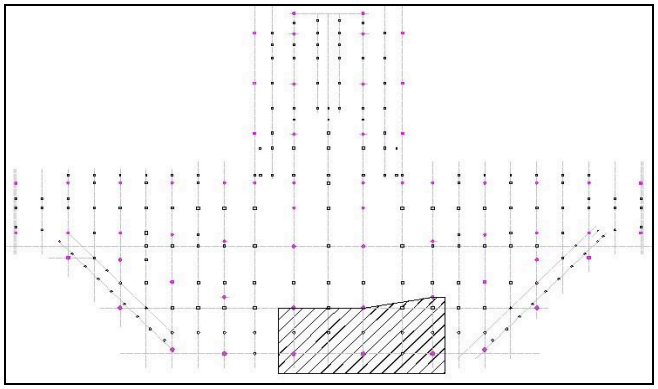

Fig. 14. Range of chord and web members around SC14 for the adjustment of sectional area (in the shaded part).

The parametric analysis results are shown in Table 7 and Table 8, including the nodal displacements and the numbers of yield and failure members, respectively. The vertical displacements of the structure after the removal of column SC14 can be effectively reduced through increasing the cross-sectional sizes of chord members, as well as the numbers of plastic members and failed members. While increasing the cross-sectional sizes of web members has little effects on the changes of structural responses. Namely, increasing the cross-sectional area of chord member is more effective to improve the progressive collapse resistance of the structure compared with web member. In addition, it should be noted that the number of failed members is reduced to 50% compared with the original structure when the chord cross-sectional sizes were enlarged to 1.15 times those of original chords. Then, the number of failed members is 0 when the amplification factor was 1.2, namely the initial failure of column SC14 will not cause further damages to other parts of the structure. Therefore, the conclusions and advices guiding the structural optimization design can be obtained through the parametric analysis. For the large-span grid structure does not meet the requirements of progressive collapse resistance, it is suggested that the cross-sectional sizes of chord members can be adjusted on the basis of meeting design requirements and codes. For the terminal building in this study, the suggested amplification factor of chord cross-sectional

area is 1.2.

Table 7

Changes of structural deformations with different sectional sizes of chord and web members (Unit: m).

Amplification factor of sectional area of member	Maximum vertical displacement after adjusting the sectional area of chord member					Maximum vertical displacement after adjusting the sectional area of web member				
	Node 8297	Node 6715	Node 6644	Node 1916	Node 6652	Node 8297	Node 6715	Node 6644	Node 1916	Node 6652
1	3.958	2.764	2.409	1.995	6.722	3.958	2.764	2.409	1.995	6.722
1.05	3.695	2.572	2.245	1.851	6.276	3.943	2.752	2.402	1.986	6.693
1.1	3.324	2.288	2.013	1.675	5.643	3.924	2.735	2.388	1.973	6.662
1.15	2.893	1.957	1.746	1.473	4.913	3.890	2.712	2.371	1.959	6.591
1.2	2.182	1.420	1.303	1.182	3.728	3.900	2.718	2.375	1.960	6.622
1.3	1.820	1.181	1.085	0.989	3.113	3.884	2.705	2.364	1.949	6.594
1.4	1.512	0.976	0.898	0.826	2.604	3.866	2.687	2.351	1.938	6.576
1.5	1.281	0.812	0.763	0.705	2.186	3.847	2.672	2.342	1.928	6.532

Table 8

Number changes of yield and failed members with different sectional sizes of chord and web members.

Amplification factor of sectional area of member	After adjusting the sectional area of chord member		After adjusting the sectional area of web member	
	Number of plastic member	Number of failed member	Number of plastic member	Number of failed member
1	590	16	590	16
1.05	543	15	589	13
1.1	462	9	604	29
1.15	418	8	581	11
1.2	307	0	594	27
1.3	246	0	597	30
1.4	205	0	577	17
1.5	184	0	569	15

Similarly, the parametric analysis for the influence of axial compression ratios of CFST columns supporting the roof on the progressive collapse resistance of the structure was carried out. The cross-sectional sizes of the CFST columns around the initial failure column SC14 were reduced in equal proportion, and the axial compression ratios of the columns were enlarged to 1~9 times those of original columns. The results show that the structural response after the removal of SC14 shows a slight increasing trend with the increases of axial compression ratios of adjacent columns. The differences of vertical displacements between the adjusted structure and original structure are less than 10%. Therefore, the change of axial compression ratio of column has little impact on the progressive collapse resistance of the structure.

7. Conclusions

In this study, we focused on the progressive collapse resistance of the terminal building of Lanzhou Zhongchuan Airport in China, which is a large-span curved spatial grid structure with main trusses. An improved method based on zoned concept judgment and sensitivity analysis was proposed to select key components. Moreover, the nonlinear time-history analyses of progressive collapse were carried out using the alternate load path method (AP method). The further optimization of the cross-sectional sizes of chord and web members of the grid structure was carried out. The significant contributions of this

study are summarized as follows:

(1) The structure has enough backup load transmission path, which can effectively prevent the progressive collapse after initial failure. The structural response after the removal of CFST column SC14 supporting the roof is the largest, the reason is that SC14 is located at the cantilever end and the column spacing is large. Most of the grid chords supported by SC14 yield, and the structure is in the state of near collapse. Therefore, the columns directly supporting the roof should be focused on for this kind of large-span spatial structure.

(2) The improved method of zoned concept judgment plus sensitivity analysis proposed in this study can effectively avoid the omission of key members. For the relatively important components with high sensitivities, the accidental loads should be further considered on the basis of meeting the requirements of code. It is suggested that the resistance levels of the upper and lower chords should be increased by 20% for the structure in this study, including the tensile strength and cross-sectional area. In addition, the changes of axial compression ratios of the columns supporting the roof have little impacts on the progressive collapse resistance of the structure.

(3) The essence of AP method is to evaluate the risk of progressive collapse of a structure, so as to enhance the structural redundancy, which cannot simulate the actual initial failure conditions of the structure. Therefore, how to reasonably simulate the effects of various unexpected loads on structure, including the progressive damage processes of components during progressive collapse, the falling processes of damaged components and the impacts on structure, and the accumulation processes of falling components, will be the main subsequent research directions, which are the lessons learned from this paper.

Competing interest

The author(s) declare no competing interests.

Acknowledgements

The authors gratefully acknowledge the Natural Science Foundation of Jiangsu Province, grant number BK20200494; Fundamental Research Funds for the Central Universities, grant number 30919011246; National Natural Science Foundation of China, grant number 51278104; Transportation Scientific Research Program of Jiangsu Province, China, grant number 2011Y03.

Author Contributions

Conceptualization, GP Zhou and QE Song; Formal analysis, GP Zhou and QE Song; Funding acquisition, GP Zhou, AQ Li, and SG Shen; Investigation, GP Zhou, QE Song, and Q Zhou; Methodology, GP Zhou and QE Song; Project administration, AQ Li and SG Shen; Software, GP Zhou, QE Song, and Q Zhou; Supervision, AQ Li and SG Shen; Validation, QE Song and Q Zhou; Writing – original draft, GP Zhou; Writing – review & editing, B Wang and YY Zhang.

References

Cai, J. G., Wang, F. L., Han, Y. L., Feng, J., Zhang, J. Practical method for the evaluation of important structural components of long-span space structures. *J. Hunan U.* **38**, 7-11; 10.1016/j.cnsns.2011.01.018 (2011).

Corley, W. G., PFM, S. R., Sozen, M. A., Thornton, C. H. The Oklahoma City Bombing: Summary and recommendations for multihazard mitigation. *J. Perform. Constr. Fac.* **12**, 100-112; 10.1061/(ASCE)0887-3828(1998)12:3(100) (1998).

Eurocode, 1. BS EN 1991-1-2005: Actions on structures Part-I: General actions-accidental actions. Brussels: CEN (2005).

Han, L. H. Concrete filled steel tubular structures. Beijing: China Science Publishing & Media Ltd (2018).

Hu, X. B., Qian, J. R. Dynamic effect analysis during progressive collapse of a single-story steel plane frame. *Eng. Mech.* **25**, 38-43; 10.1016/S1872-5791(08)60058-5 (2008).

Kaewkulchai, G., Williamson, E. B. Beam element formulation and solution procedure for dynamic progressive collapse analysis. *Comput. Struct*. **82,** 639-651; 10.1016/j.compstruc.2003.12.001 (2004).

LéGeron, F. D. R., Paultre, P. Uniaxial confinement model for normal and high-strength concrete columns. *J. Struct. Eng.* **129**, 241-252; 10.1061/(ASCE)0733-9445(2003)129:2(241) (2003).

Li, G. Q,. Sun, J. Y., Wang, K. Q. Research on a simplified frame column model to resist blast load. *J. Vib. Shock.* **26**, 8-13; 10.1016/S0252-9602(07)60014-9 (2007).

Li, Y. Study on design method for RC frame structures to resist progressive collapse. *Tsinghua Univ.* (2011).

Longinow, A., Mniszewski, K. R. Protecting buildings against vehicle bomb attacks. *Pract. Period. Struct. Des. Construct.* **1**, 51-54; 10.1061/(ASCE)1084-0680(1996)1:1(51) (1996).

Lu, X. Z., Li, Y., Ye, L.P., et al. Study on design method to resist progressive collapse for reinforced concrete frames. *Eng. Mech.* **25**, 150-157; 10.3969/j.issn.1002-5944.2017.18.096 (2008).

Marjanishvili, S., Agnew, E. Comparison of various procedures for progressive collapse analysis. *J. Perform. Constr. Fac.* **20**, 365-374; 10.1061/(ASCE)0887-3828(2006)20:4(365) (2006).

Shi, Y. C., Li, Z. X., Hao, H. Numerical analysis of progressive collapse of reinforced concrete frame under blast loading. *J. PLA U. Sci. Tech.* **8**, 652-658; 10.7666/j.issn.1009-3443.20070617 (2007).

Ye, L. P., Lu, X. Z., Ma, Q. L., Wang, X. L., Miao, Z. W. Seismic nonlinear analytical models, methods and examples for concrete structures. *Eng. Mech.* **23**, 131-140; 10.3969/j.issn.1000-4750.2006.z2.013 (2006).

Zhang, L. M., Liu, X. L. Network of energy transfer in frame structures and its preliminary application. *China. Civil. Eng. J.* **40**, 45-49; 10.1016/S1672-6529(07)60007-9 (2007).

Zhou, J., Chen, S. W., Su, J., et al. Progressive collapse analysis of a building in Hongqiao communication junction. *J. Build. Struct.* **31**, 174-180; CNKI:SUN:JZJB.0.2010-05-025 (2010).